A Reynolds–uniform numerical method for Prandtl's boundary layer problem for flow past a wedge

J.S. Butler

Department of Mathematics, Trinity College, Dublin, Ireland.

J.J.H Miller

Department of Mathematics, Trinity College, Dublin, Ireland

G.I. Shishkin

Institute for Mathematics and Mechanics, Russian Academy of Sciences, Ekaterinburg, Russia

Abstract

In this paper we deal with Prandtl's boundary layer problem for incompressible laminar flow past a wedge. When the Reynolds number is large the solution of this problem has a parabolic boundary layer. We construct a direct numerical method for computing approximations to the solution of this problem using a piecewise uniform fitted mesh technique appropriate to the parabolic boundary layer. We use the numerical method to approximate the self–similar solution of Prandtl's problem in a finite rectangle excluding the leading edge of the wedge, which is the source of an additional singularity caused by incompatibility of the problem data. We verify that the constructed numerical method is robust in the sense that the computed errors for the velocity components and their derivatives in the discrete maximum norm are Reynolds uniform. We construct and apply a special numerical method related to the Falkner–Skan technique to compute a reference solution for the error analysis of the velocity components and their derivatives. By means of extensive numerical experiments we show that the constructed direct numerical method is Reynolds–uniform.

1 Introduction

Incompressible laminar flow past a semi-infinite wedge W in the domain D = $\mathbf{R}^2$ / W is governed by the Navier-Stokes equations. Using Prandtl's approach the vertical momentum equation is omitted and the horizontal momentum equation is simplified , see [2]and [3]. The new momentum equation is parabolic and singularly perturbed, which means that the highest order derivative is multiplied by a small singular perturbation parameter. In this case the parameter is the reciprocal of the Reynolds number. For convenience we use the notation $\varepsilon = \frac{1}{Re}$.

It is well known that for flow problems with large Reynolds numbers a boundary layer arises on the surface of the wedge. Also, when classical numerical methods are applied to these problems large errors occur, especially in approximations of the derivatives, which grow unboundedly as the Reynolds number increases. For this reason robust layer-resolving numerical methods, in which the error is independent of the singular perturbation parameter, are required. We want to solve the Prandtl problem in a region including the parabolic boundary layer. Since the solution of the problem has another singularity at the leading edge of the wedge

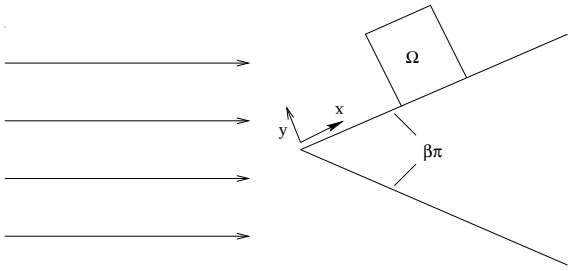

Figure 1: Flow past a wedge

we take as the computational domain the finite rectangle $\Omega = (.1, 1.1) \times (0, 1)$ on the upper side of the wedge, which sufficiently far from the leading edge (see fig. 1) that the leading edge singularity does not cause problems for the numerical method . We denote the boundary of Ω by $\Gamma = \Gamma_L \bigcup \Gamma_T \bigcup \Gamma_B \bigcup \Gamma_R$ where Γ_L, Γ_T, Γ_B and Γ_R denote, respectively the left-hand, top, bottom and right-hand edges of Ω.

The Prandtl boundary layer problem in D is:

$$(P_\varepsilon)\begin{cases} \text{Find } \mathbf{u}_\varepsilon = (u_\varepsilon, v_\varepsilon) \text{ such that for all } (x,y) \in D \\ \\ \mathbf{u}_\varepsilon \text{ satisfies the differential equation} \\ \\ -\frac{1}{Re}\frac{\partial^2 u_\varepsilon}{\partial^2 y} + \mathbf{u}_\varepsilon.\nabla u_\varepsilon = U\frac{dU}{dx} \\ \\ \nabla.\mathbf{u}_\varepsilon = 0 \\ \\ \text{with boundary conditions} \\ \\ \mathbf{u}_\varepsilon = 0 \text{ on } \Gamma_B \\ \\ \mathbf{u}_\varepsilon = \mathbf{u}_P \text{ on } \Gamma_L \bigcup \Gamma_T \end{cases}$$

where $m = \frac{\beta}{2-\beta}$, $\beta\pi$ is the angle in radians of the wedge and $U(x) = x^m$.

Our goal is to construct a numerical method for which there are error bounds for the solution components and their derivatives, which do not depend on the value of Re or β, for $Re \in [1,\infty)$ and $\beta \in [0,1]$. That is the method is (Re,β)–uniform.

2 Falkner–Skan solution

Using the transformation described in [4], (P_ε) can be simplified to the well–known Falkner–Skan problem, involving a non-linear ordinary differential equation, which we now describe. Writing

$$\eta = y\sqrt{\frac{(m+1)Re}{2}\frac{U}{x}}$$

the velocity components have the form

$$u_{FS}(x,y) = u_1 x^m f'(\eta) = U f'(\eta)$$

$$v_{FS}(x,y) = -\sqrt{\frac{m+1}{2x}\frac{U}{Re}}\left(f + \frac{m-1}{m+1}\eta f'\right).$$

where f is the solution of the Falkner–Skan problem

$$(P_{FS})\begin{cases} \text{For } \eta \in (0,\infty) \text{ find } f \in C^3(0,\infty) \\ \\ f''' + ff'' + \beta(1-f'^2) = 0 \\ \\ \text{with boundary conditions} \\ \\ f(0) = f'(0) = 0, \qquad\qquad f'(\infty) = 1. \end{cases}$$

To find the components $u_{FS}(x,y)$, $v_{FS}(x,y)$ of $\mathbf{u_{FS}}$, and their derivatives, we need to solve (P_{FS})numerically for $f(\eta)$ and its derivatives on the semi-infinite domain [0,∞) and then we apply post-processing to determine numerical

approximations to $\mathbf{u}_\varepsilon$. This process is described in detail in [1] for flow past a flat plate.

The purpose of finding this Falkner–Skan solution of Prandtl's problem is that we use it as a reference solution for the unknown exact solution in the expression for the error, when we estimate the error in the direct method of the next section. In this way, since the Falkner–Skan solution is known to converge Reynolds–uniformly to the solution of Prandtl's problem and we can estimate guaranteed error bounds for it. For this purpose we use the Falkner–Skan solution for (P_{FS}) when N=8192, namely $\mathbf{U}_{FS}^{8192}$, which provides the required accuracy for the velocity components U_{FS}^{8192}, V_{FS}^{8192} and their derivatives $D_x V_{FS}^{8192}$, $D_y V_{FS}^{8192}$ and their scaled derivative $\sqrt{\varepsilon} D_y U_{FS}^{8192}$.

3 Prandtl's Problem

The aim of this section is to construct a robust numerical method to solve the Prandtl problem (P_ε) for all admissible values of β and Reynolds numbers Re.

When constructing a mesh in the rectangle Ω, it is important to note where the boundary layer occurs in order to define an appropriate transition point from the coarse to the fine mesh. We define the mesh as a tensor product of two one–dimensional meshes. The mesh in the x direction is the uniform mesh (see fig. 2)

$$\Omega_\varepsilon^{N_x} = \{x_i : x_i = 0.1 + iN_x^{-1}, 0 \leq i \leq N_x\}.$$

The mesh in the y-direction is a piecewise–uniform fitted mesh, which is defined by

$$\Omega_\varepsilon^{N_y} = \{y_j : y_j = \sigma j \frac{2}{N_y}, 0 \leq j \leq \frac{N_y}{2}; y_j = \sigma + (1-\sigma)(j - \frac{N_y}{2})\frac{2}{N_y}, \frac{N_y}{2} \leq j \leq N_y\}$$

The transition point σ is chosen so that there is a fine mesh in the boundary layer when required. The appropriate choice in this case is

$$\sigma = \min\{\frac{1}{2}, \sqrt{\varepsilon} ln N_y\}.$$

The factor $\sqrt{\varepsilon}$ may be motivated from *a priori* estimates of the derivatives of the solution $\mathbf{u}_\varepsilon$ or from asymptotic analysis. The rectangular mesh is then the tensor product $\Omega_\varepsilon^{\mathbf{N}} = \Omega_\varepsilon^{N_x} \times \Omega_\varepsilon^{N_y}$, where $\mathbf{N}$=(N_x, N_y). For simplicity we take $N_x = N_y = N$.

The problem (P_ε) is discretized by the following non-linear upwind finite

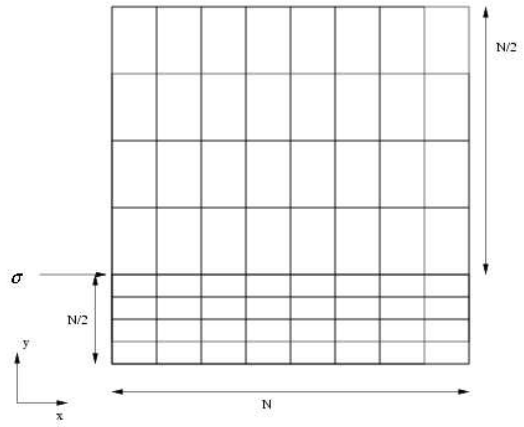

Figure 2: 2-d mesh constructed from a tensor product

difference method on the piecewise uniform fitted mesh $\Omega_\varepsilon^{\mathbf{N}}$

$$(P_\varepsilon^{\mathbf{N}}) \begin{cases} \text{Find } \mathbf{U}_\varepsilon = (U_\varepsilon, V_\varepsilon) \text{ such that for all } (x_i, y_j) \in \Omega_\varepsilon^{\mathbf{N}} \\ \mathbf{U}_\varepsilon \text{ satisfies the finite difference equations} \\ -\varepsilon \delta_y^2 U_\varepsilon(x_i, y_j) + U_\varepsilon(x_i, y_j) D_x^- U_\varepsilon(x_i, y_j) + \\ V_\varepsilon(x_i, y_j) D_y^u U_\varepsilon(x_i, y_j) = U(x_i) \frac{dU}{dx}(x_i) \\ D_x^- U_\varepsilon(x_i, y_j) + D_y^- V_\varepsilon(x_i, y_j) = 0 \\ \text{with boundary conditions} \\ \mathbf{U}_\varepsilon = 0 \text{ on } \Gamma_B \\ \mathbf{U}_\varepsilon = \mathbf{U}_{FS} \text{ on } \Gamma_L \bigcup \Gamma_T \end{cases}$$

where, for any continuous function $V_\varepsilon(x_i, y_j)$ on the domain $\Omega_\varepsilon^{\mathbf{N}}$, D_y^u is defined by

$$V_\varepsilon(x_i, y_j) D_y^u U_\varepsilon(x_i, y_j) = \begin{cases} V_\varepsilon(x_i, y_j) D_y^- U_\varepsilon(x_i, y_j) & \text{if } V_\varepsilon(x_i, y_j) \geq 0; \\ V_\varepsilon(x_i, y_j) D_y^+ U_\varepsilon(x_i, y_j) & \text{if } V_\varepsilon(x_i, y_j) < 0. \end{cases}$$

δ_y^2 is the standard second order centered difference operator in the y direction, D_x^-, D_x^+ and D_y^-, D_y^+ are the standard first order backward, respectively forward, finite difference operators in the x and y directions.

The need to change between forward and backward differences is due to the fact that, at angles $\beta > 0.1$, V_ε is initially negative and then becomes positive. Therefore, without these changes, the tridiagonal system is no longer diagonally

dominant and the continuation algorithm fails to converge.

Since the problem $(P_\varepsilon^{\mathbf{N}})$ is a nonlinear system an iterative method is required for its solution. This is obtained by replacing the system of nonlinear equations with a sequence of systems of linear equations. The systems of linearized equations are

$$(A_\varepsilon^{\mathbf{N}}) \begin{cases} \text{With the boundary condition } \mathbf{U}_\varepsilon^{\mathbf{M}} = \mathbf{U}_{\mathrm{FS}}^{\mathbf{8192}} \text{ on } \Gamma_{\mathrm{L}}, \\ \text{for each } i, 1 \le i \le N, \text{ use the initial guess } \mathbf{U}_\varepsilon^0|_{X_i} = \mathbf{U}_\varepsilon^{M_{i-1}}|_{X_{i-1}} \\ \text{and for } m = 1, \ldots, M_i \text{ solve the following} \\ \text{two point boundary value problem for } U_\varepsilon^m(x_i, y_j) \\ (-\varepsilon\delta_y^2 + \mathbf{U}_\varepsilon^{m-1} \cdot \mathbf{D}^-)U_\varepsilon^m(x_i, y_j) = (U\tfrac{dU}{dx})(x_i), \quad 1 \le j \le N-1 \\ \text{with the boundary conditions } U_\varepsilon^m = U_{\mathrm{FS}} \text{ on } \Gamma_{\mathrm{B}} \cup \Gamma_{\mathrm{T}}, \\ \text{and the initial guess for } V_\varepsilon^0|_{X_1} = 0. \\ \text{Also solve the initial value problem for } V_\varepsilon^m(x_i, y_j) \\ (\mathbf{D}^- \cdot \mathbf{U}_\varepsilon^m)(x_i, y_j) = 0, \\ \text{with initial condition } V_\varepsilon^m = 0 \text{ on } \Gamma_{\mathrm{B}}. \\ \text{Continue to iterate between the equations for } \mathbf{U}_\varepsilon^m \text{ until } m = M_i, \\ \text{where } M_i \text{ is such that} \\ \max\big(|U_\varepsilon^{M_i} - U_\varepsilon^{M_i-1}|_{\overline{X}_i}, \tfrac{1}{V^*}|V_\varepsilon^{M_i} - V_\varepsilon^{M_i-1}|_{\overline{X}_i}\big) \le tol. \end{cases}$$

For notational simplicity, we suppress explicit mention of the iteration superscript M_i henceforth, and we write simply $\mathbf{U}_\varepsilon$ for the solution generated by $(A_\varepsilon^{\mathbf{N}})$. We take $tol = 10^{-6}$ in the computations. We note that there are no known theoretical results concerning the convergence of the solutions $\mathbf{U}_\varepsilon$ of $(P_\varepsilon^{\mathbf{N}})$ to the solution $\mathbf{u}_\varepsilon$ of (P_ε) and no theoretical estimate for the pointwise error $(\mathbf{U}_\varepsilon - \mathbf{u}_\varepsilon)(x_i, y_j)$. It is for this reason that we are forced to apply controllable experimental techniques, which are adapted to the problem under consideration and are of crucial value to our understanding of the computationally problems. V^* is defined to be

$$V^* = \max_{\Omega_\varepsilon^N} V_{FS}.$$

4 Error Analysis

In this section we compute Reynolds–uniform maximum pointwise errors in the approximations generated by the direct numerical method described in the previous section. For the sake the brevity, we show the errors for only one typical value of the angle of the wedge, $\beta = 0.6$.

For this case we compare the parameter uniform maximum pointwise errors in the approximations generated by the direct numerical method of the previous section with the corresponding values of U_{FS}^{8192}. We use the following definitions for the errors

$$E_\varepsilon^{\mathbf{N}}(U_\varepsilon) = ||U_\varepsilon - \overline{U_{FS}}^{8192}||_{\overline{\Omega}_\varepsilon^N}$$

$$E_\varepsilon^{\mathbf{N}}(\frac{1}{V^*}V_\varepsilon) = \frac{1}{V^*}||V_\varepsilon - \overline{V_{FS}}^{8192}||_{\overline{\Omega}_\varepsilon^N}$$

The results in Tables 1 and 2 indicate that the method is Reynolds–uniform for the scaled velocities.

$\varepsilon\backslash N$	8	16	32	64	128	256	512
2^{-0}	1.80e-03	1.34e-03	7.58e-04	4.33e-04	2.36e-04	1.29e-04	6.98e-05
2^{-2}	1.39e-02	8.19e-03	4.51e-03	2.40e-03	1.24e-03	6.30e-04	3.16e-04
2^{-4}	3.00e-02	1.66e-02	8.87e-03	4.59e-03	2.33e-03	1.17e-03	5.83e-04
2^{-6}	3.39e-02	2.04e-02	1.10e-02	5.69e-03	2.87e-03	1.43e-03	7.11e-04
2^{-8}	3.32e-02	1.99e-02	1.12e-02	5.82e-03	2.98e-03	1.51e-03	7.65e-04
2^{-10}	3.34e-02	1.93e-02	1.11e-02	5.82e-03	2.98e-03	1.51e-03	7.65e-04
2^{-12}	3.81e-02	1.93e-02	1.10e-02	5.81e-03	2.98e-03	1.51e-03	7.65e-04
2^{-14}	4.62e-02	1.93e-02	1.10e-02	5.81e-03	2.98e-03	1.51e-03	7.65e-04
2^{-16}	5.05e-02	1.93e-02	1.10e-02	5.81e-03	2.98e-03	1.51e-03	7.65e-04
2^{-18}	5.26e-02	1.93e-02	1.09e-02	5.81e-03	2.98e-03	1.51e-03	7.65e-04
2^{-20}	5.37e-02	1.93e-02	1.09e-02	5.81e-03	2.98e-03	1.51e-03	7.65e-04
E^N	5.37e-02	2.04e-02	1.12e-02	5.82e-03	2.98e-03	1.51e-03	7.65e-04

Table 1: Computed maximum pointwise error $E_\varepsilon^{\mathbf{N}}(U_\varepsilon)$ where U_ε is generated by $(A_\varepsilon^{\mathbf{N}})$ for various values of ε, N and β=0.6.

$\varepsilon\backslash N$	8	16	32	64	128	256	512
2^{-0}	2.67e-01	1.77e-01	9.95e-02	5.25e-02	2.79e-02	1.50e-02	8.28e-03
2^{-2}	1.89e-01	1.07e-01	5.39e-02	2.76e-02	1.41e-02	7.32e-03	3.88e-03
2^{-4}	1.28e-01	7.11e-02	3.52e-02	1.78e-02	9.02e-03	4.61e-03	2.39e-03
2^{-6}	9.82e-02	5.51e-02	2.85e-02	1.51e-02	7.65e-03	3.88e-03	1.98e-03
2^{-8}	8.60e-02	4.53e-02	2.21e-02	1.15e-02	6.02e-03	3.17e-03	1.67e-03
2^{-10}	8.00e-02	4.09e-02	1.93e-02	9.75e-03	5.02e-03	2.59e-03	1.33e-03
2^{-12}	7.69e-02	3.88e-02	1.79e-02	8.95e-03	4.55e-03	2.31e-03	1.18e-03
2^{-14}	7.54e-02	3.77e-02	1.72e-02	8.57e-03	4.32e-03	2.18e-03	1.10e-03
2^{-16}	7.46e-02	3.72e-02	1.69e-02	8.37e-03	4.20e-03	2.11e-03	1.06e-03
2^{-18}	7.42e-02	3.70e-02	1.68e-02	8.28e-03	4.15e-03	2.08e-03	1.04e-03
2^{-20}	7.40e-02	3.68e-02	1.67e-02	8.23e-03	4.12e-03	2.07e-03	1.04e-03
E^N	2.67e-01	1.77e-01	9.95e-02	5.25e-02	2.79e-02	1.50e-02	8.28e-03

Table 2: Computed maximum pointwise error $E_\varepsilon^{\mathbf{N}}(\frac{1}{V^*}V_\varepsilon)$ where V_ε is generated by $(A_\varepsilon^{\mathbf{N}})$ for various values of ε, N and β=0.6.

In fig. 3 we see that the computed scaled velocity components have no non-physical oscillations. The boundary layer at the wedge is apparent for the horizontal velocity component U_ε.

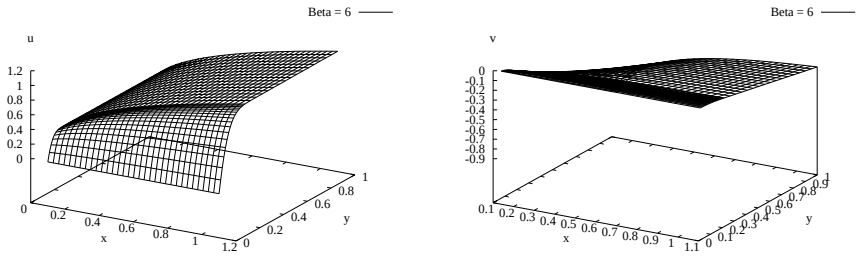

Figure 3: Graphs of U_ε and $\frac{1}{V^*}V_\varepsilon$ for $\varepsilon = 2^{-8}$, N=32 and $\beta = 0.6$

In Tables 3 and 4 we give the computed orders of convergence for the velocity components. We define $p^N_{\varepsilon,comp}$ by

$$p^N_{\varepsilon,comp} = log_2 \frac{||U^N_\varepsilon - U^{8192}_{FS}||_{\Omega^N_\varepsilon}}{||U^{2N}_\varepsilon - U^{8192}_{FS}||_{\Omega^{2N}_\varepsilon}}$$

and p^N_{comp} by

$$p^N_{comp} = log_2 \frac{max_\varepsilon ||U^N_\varepsilon - U^{8192}_{FS}||_{\Omega^N_\varepsilon}}{max_\varepsilon ||U^{2N}_\varepsilon - U^{8192}_{FS}||_{\Omega^{2N}_\varepsilon}}.$$

$\varepsilon \backslash N$	8	16	32	64	128	256
2^{-0}	0.42	0.82	0.81	0.87	0.88	0.88
2^{-2}	0.76	0.86	0.91	0.95	0.98	0.99
2^{-4}	0.85	0.91	0.95	0.98	0.99	1.01
2^{-6}	0.73	0.89	0.95	0.99	1.00	1.01
2^{-8}	0.74	0.83	0.94	0.97	0.98	0.99
2^{-10}	0.79	0.80	0.93	0.97	0.98	0.99
2^{-12}	0.98	0.81	0.92	0.96	0.98	0.99
2^{-14}	1.26	0.81	0.92	0.96	0.98	0.99
2^{-16}	1.39	0.82	0.92	0.96	0.98	0.99
2^{-18}	1.45	0.82	0.91	0.96	0.98	0.99
2^{-20}	1.48	0.82	0.91	0.96	0.98	0.99
p^N_{comp}	1.40	0.86	0.94	0.97	0.98	0.99

Table 3: Computed orders of convergence $p^N_{\varepsilon,comp}$, p^N_{comp} for $U_\varepsilon - U^{8192}_{FS}$ where U_ε is generated by $(A^{\mathbf{N}}_\varepsilon)$ for various values of ε, N and β=0.6.

$\varepsilon \backslash N$	8	16	32	64	128	256
2^{-0}	0.59	0.83	0.92	0.91	0.90	0.86
2^{-2}	0.82	0.99	0.97	0.96	0.95	0.92
2^{-4}	0.84	1.02	0.99	0.98	0.97	0.95
2^{-6}	0.84	0.95	0.91	0.98	0.98	0.97
2^{-8}	0.92	1.03	0.95	0.93	0.93	0.93
2^{-10}	0.97	1.09	0.98	0.96	0.96	0.96
2^{-12}	0.99	1.11	1.00	0.98	0.98	0.97
2^{-14}	1.00	1.13	1.01	0.99	0.99	0.99
2^{-16}	1.00	1.14	1.01	0.99	0.99	0.99
2^{-18}	1.01	1.14	1.02	1.00	0.99	1.00
2^{-20}	1.01	1.14	1.02	1.00	1.00	1.00
p^N_{comp}	0.59	0.83	0.92	0.91	0.90	0.86

Table 4: Computed orders of convergence $p^N_{\varepsilon,comp}$, p^N_{comp} for $\frac{1}{V^*}(V_\varepsilon - V^{8192}_{FS})$ where V_ε is generated by $(A^{\mathbf{N}}_\varepsilon)$ for various values of ε, N and β=0.6.

From these tables we see that for all $N \geq 16$ the order of convergence for the approximations to the scaled velocity components in each case is at least 0.78. Thus we have shown that for the velocity components the methods is Reynolds uniform for $\beta = 0.6$.

The graphs in fig. 4 show where the error in the scaled velocity components is largest. For the horizontal component this is at points in the boundary layer and for the vertical component it is at points farthest from the surface of the wedge.

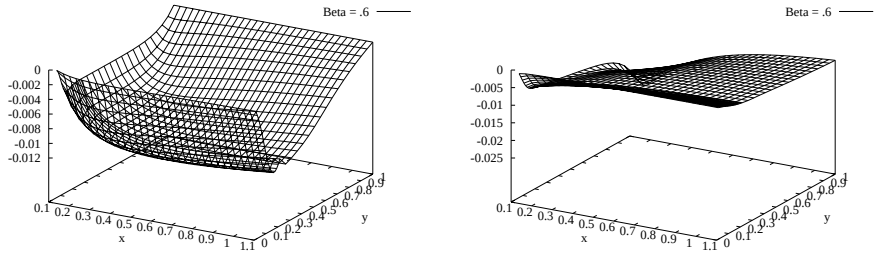

Figure 4: Graphs of $U_\varepsilon - U_{FS}$ and $\frac{1}{V^*}(V_\varepsilon - V_{FS})$ for $\varepsilon = 2^{-8}$, N=32 and $\beta = 0.6$.

In Tables 5-7 we display the computed maximum pointwise errors of the approximations to the scaled first order derivatives of the velocity components. Since $D_y V = -D_x U$ it is only necessary to show the errors for one of them. Further computations, not reported here, show that the errors for the scaled derivatives reduce as the angle β tends to 1, because the singularity at the leading edge has less effect. From these numerical experiments it follows that the method is (Re, β)-uniform.

$\varepsilon\backslash N$	8	16	32	64	128	256	512
2^{-0}	3.73e-02	1.91e-02	1.04e-02	5.52e-03	2.91e-03	1.55e-03	8.49e-04
2^{-2}	7.35e-02	3.73e-02	1.88e-02	9.51e-03	4.87e-03	2.54e-03	1.38e-03
2^{-4}	1.39e-01	7.35e-02	3.73e-02	1.88e-02	9.51e-03	4.87e-03	2.54e-03
2^{-6}	1.44e-01	1.00e-01	6.40e-02	3.73e-02	1.90e-02	9.61e-03	4.90e-03
2^{-8}	1.44e-01	1.00e-01	6.40e-02	3.87e-02	2.30e-02	1.33e-02	7.56e-03
2^{-10}	1.44e-01	1.00e-01	6.40e-02	3.87e-02	2.30e-02	1.33e-02	7.56e-03
2^{-12}	1.44e-01	1.00e-01	6.40e-02	3.87e-02	2.30e-02	1.33e-02	7.56e-03
2^{-14}	1.44e-01	1.00e-01	6.40e-02	3.87e-02	2.30e-02	1.33e-02	7.56e-03
2^{-16}	1.44e-01	1.00e-01	6.40e-02	3.87e-02	2.30e-02	1.33e-02	7.56e-03
2^{-18}	1.44e-01	1.00e-01	6.40e-02	3.87e-02	2.30e-02	1.33e-02	7.56e-03
2^{-20}	1.44e-01	1.00e-01	6.40e-02	3.87e-02	2.30e-02	1.33e-02	7.56e-03
E^N	1.44e-01	1.00e-01	6.40e-02	3.87e-02	2.30e-02	1.33e-02	7.56e-03

Table 5: Computed maximum pointwise scaled error $\sqrt{\varepsilon}||D_y^- U_\varepsilon - D_y U_{FS}^{8192}||_{\overline{\Omega_\varepsilon^N}/\Gamma_L}$ where U_ε is generated by $(A_\varepsilon^{\mathbf{N}})$ for various values of ε, N and β=.6.

$\varepsilon\backslash N$	8	16	32	64	128	256	512
2^{-0}	2.09e-01	1.58e-01	1.03e-01	5.98e-02	3.24e-02	1.68e-02	8.45e-03
2^{-2}	2.55e-01	1.81e-01	1.13e-01	6.44e-02	3.45e-02	1.79e-02	9.11e-03
2^{-4}	2.79e-01	1.69e-01	1.07e-01	6.12e-02	3.29e-02	1.71e-02	8.74e-03
2^{-6}	2.92e-01	2.08e-01	1.31e-01	7.63e-02	3.86e-02	1.98e-02	1.04e-02
2^{-8}	2.92e-01	2.08e-01	1.31e-01	7.92e-02	4.66e-02	2.71e-02	1.56e-02
2^{-10}	2.92e-01	2.08e-01	1.31e-01	7.92e-02	4.66e-02	2.71e-02	1.56e-02
2^{-12}	2.92e-01	2.08e-01	1.31e-01	7.92e-02	4.66e-02	2.71e-02	1.56e-02
2^{-14}	2.92e-01	2.08e-01	1.31e-01	7.92e-02	4.66e-02	2.71e-02	1.56e-02
2^{-16}	2.92e-01	2.08e-01	1.31e-01	7.92e-02	4.66e-02	2.71e-02	1.56e-02
2^{-18}	2.92e-01	2.08e-01	1.31e-01	7.92e-02	4.66e-02	2.71e-02	1.56e-02
2^{-20}	2.92e-01	2.08e-01	1.31e-01	7.92e-02	4.66e-02	2.71e-02	1.56e-02
E^N	2.92e-01	2.08e-01	1.31e-01	7.92e-02	4.66e-02	2.71e-02	1.56e-02

Table 6: Computed maximum pointwise error $||D_y^- V_\varepsilon - D_y V_{FS}^{8192}||_{\overline{\Omega_\varepsilon^N}}$ where V_ε is generated by $(A_\varepsilon^{\mathbf{N}})$ for various values of ε, N and β=.6.

$\varepsilon\backslash N$	8	16	32	64	128	256	512
2^{-0}	1.50e+00	1.59e+00	1.12e+00	6.58e-01	3.74e-01	2.55e-01	3.78e-01
2^{-2}	8.75e-01	8.23e-01	6.22e-01	3.93e-01	2.50e-01	1.75e-01	8.49e-02
2^{-4}	6.43e-01	6.64e-01	5.49e-01	3.80e-01	2.55e-01	1.78e-01	1.05e-01
2^{-6}	5.89e-01	6.03e-01	5.05e-01	3.66e-01	2.58e-01	1.85e-01	1.26e-01
2^{-8}	5.68e-01	5.72e-01	4.64e-01	3.19e-01	2.21e-01	1.59e-01	1.14e-01
2^{-10}	5.60e-01	5.59e-01	4.46e-01	2.95e-01	1.93e-01	1.29e-01	8.42e-02
2^{-12}	5.57e-01	5.53e-01	4.37e-01	2.84e-01	1.79e-01	1.14e-01	6.99e-02
2^{-14}	5.56e-01	5.50e-01	4.33e-01	2.78e-01	1.72e-01	1.07e-01	6.28e-02
2^{-16}	5.56e-01	5.48e-01	4.30e-01	2.75e-01	1.68e-01	1.04e-01	5.93e-02
2^{-18}	5.55e-01	5.48e-01	4.29e-01	2.74e-01	1.67e-01	1.02e-01	5.76e-02
2^{-20}	5.55e-01	5.47e-01	4.29e-01	2.73e-01	1.66e-01	1.01e-01	5.67e-02
E^N	1.50e+00	1.59e+00	1.12e+00	6.58e-01	3.74e-01	2.55e-01	3.78e-01

Table 7: Computed maximum pointwise scaled error $V^{*-1}||D_x^- V_\varepsilon - D_x V_{FS}^{8192}||_{\overline{\Omega_\varepsilon^N}}$ where V_ε is generated by $(A_\varepsilon^{\mathbf{N}})$ for various values of ε, N and β=.6.

In Tables 8 -?? we display the computed orders of convergence for the approximations of the first order derivatives of the velocity components $D_x^- V_\varepsilon, D_y^- V_\varepsilon$ and scaled derivative $\sqrt{\varepsilon} D_y^- U_\varepsilon$ obtained respectively from the corresponding Tables 5-7. We see that for each value of N the orders of convergence stabilize as $\varepsilon \to 0$ for $\beta = 0.6$. Similar behavior is observed for all $\beta \in [0, 1]$.

$\varepsilon \backslash N$	8	16	32	64	128	256
2^{-0}	0.97	0.87	0.91	0.92	0.91	0.87
2^{-2}	0.98	0.99	0.98	0.97	0.94	0.88
2^{-4}	0.92	0.98	0.99	0.98	0.97	0.94
2^{-6}	0.52	0.65	0.78	0.98	0.98	0.97
2^{-8}	0.52	0.65	0.72	0.75	0.79	0.81
2^{-10}	0.52	0.65	0.72	0.75	0.79	0.81
2^{-12}	0.52	0.65	0.72	0.75	0.79	0.81
2^{-14}	0.52	0.65	0.72	0.75	0.79	0.81
2^{-16}	0.52	0.65	0.72	0.75	0.79	0.81
2^{-18}	0.52	0.65	0.72	0.75	0.79	0.81
2^{-20}	0.52	0.65	0.72	0.75	0.79	0.81
p_{comp}^N	0.52	0.65	0.72	0.75	0.79	0.81

Table 8: Computed orders of convergence $p_{\varepsilon,comp}^N$, p_{comp}^N for $\sqrt{\varepsilon}(D_y^- U_\varepsilon - D_y U_{FS}^{8192})$ where U_ε is generated by $(A_\varepsilon^{\mathbf{N}})$ for various values of ε, N and β=0.6.

$\varepsilon \backslash N$	8	16	32	64	128	256
2^{-0}	0.40	0.62	0.78	0.89	0.95	0.99
2^{-2}	0.49	0.68	0.81	0.90	0.95	0.97
2^{-4}	0.72	0.66	0.80	0.89	0.94	0.97
2^{-6}	0.49	0.67	0.78	0.98	0.96	0.92
2^{-8}	0.49	0.67	0.73	0.76	0.79	0.79
2^{-10}	0.49	0.67	0.73	0.76	0.79	0.79
2^{-12}	0.49	0.67	0.73	0.76	0.79	0.79
2^{-14}	0.49	0.67	0.73	0.76	0.79	0.79
2^{-16}	0.49	0.67	0.73	0.76	0.79	0.79
2^{-18}	0.49	0.67	0.73	0.76	0.79	0.79
2^{-20}	0.49	0.67	0.73	0.76	0.79	0.79
p_{comp}^N	0.49	0.67	0.73	0.76	0.79	0.79

Table 9: Computed orders of convergence $p_{\varepsilon,comp}^N$, p_{comp}^N for $D_y^- V_\varepsilon - D_y V_{FS}^{8192}$ where V_ε is generated by $(A_\varepsilon^{\mathbf{N}})$ for various values of ε, N and β=0.6.

$\varepsilon \backslash N$	8	16	32	64	128	256
2^{-2}	0.09	0.40	0.66	0.66	0.51	1.05
2^{-4}	-0.05	0.27	0.53	0.58	0.51	0.77
2^{-6}	-0.03	0.26	0.47	0.50	0.48	0.55
2^{-8}	-0.01	0.30	0.54	0.53	0.48	0.48
2^{-10}	0.00	0.33	0.60	0.61	0.58	0.62
2^{-12}	0.01	0.34	0.62	0.67	0.64	0.71
2^{-14}	0.02	0.35	0.64	0.70	0.68	0.77
2^{-16}	0.02	0.35	0.64	0.71	0.70	0.80
2^{-18}	0.02	0.35	0.65	0.72	0.71	0.82
2^{-20}	0.02	0.35	0.65	0.72	0.72	0.83
p^N_{comp}	-0.08	0.51	0.76	0.82	0.55	0.54

Table 10: Computed orders of convergence $p^N_{\varepsilon,comp}$, p^N_{comp} for $\frac{1}{V^*}(D_x^- V_\varepsilon - D_x V_{FS}^{8192})$ where V_ε is generated by $(A_\varepsilon^{\mathbf{N}})$ for various values of ε, N and β=0.6.

5 Conclusion

We considered Prandtl's boundary layer equations for incompressible laminar flow past a wedge with angle $\beta\pi$, $\beta \in [0,1]$. When the Reynolds number is large the solution of this problem has a parabolic boundary layer. We constructed a direct numerical method for computing approximations to the solution of this problem using a piecewise uniform fitted mesh technique appropriate to the parabolic boundary layer. We used the method to approximate the self–similar solution of Prandtl's problem in a finite rectangle excluding the leading edge of the wedge for various values of Re and β. To analyse the efficiency of the constructed we constructed and applied a special numerical method related to the Falkner–Skan technique to compute reference solutions for the error analysis of the velocity components and their derivatives. By means of extensive numerical experiments we showed that the constructed direct numerical method is Reynolds and β uniform.

ACKNOWLEDGMENTS

This research was supported in part by the Enterprise Ireland grants SC-98-612 and SC/2000/070/ and by the Russian Foundation for Basic Research under grant No. 01-01-01022.

References

[1] P. Farrell, A Hegarty, J.J.H. Miller, E. O'Riordan, G.I. Shishkin, *Robust Computational Techniques for Boundary Layers*, CRC Press, (2000).

[2] H. Schlichting, *Boundary Layer Theory*, 7^{th} edition, McGraw Hill, (1951).

[3] D.J. Acheson, *Elementary Fluid Dynamics*, Oxford: Clarendon, (1990).

[4] D.F. Rogers, *Laminar Flow Analysis*, Cambridge University Press, (1992).